4 Microscopic modeling of highway traffic

In Chapter 3 a detailed description of the microscopic driving behavior in the various traffic states has been provided. It turned out that differences of the elementary dynamics of the vehicles become most obvious in observables like the time-headway and the mean velocity at a given headway. But even the fundamental diagram reveals the existence of three distinct traffic states.
A quite realistic flow-density relation can already be obtained by the CA model of Nagel and Schreckenberg [106] (hereafter cited as NaSch model). Furthermore, spontaneous jam formation has been observed in the model. Thereby the NaSch model is a minimal model in the sense that any further simplification of the model leads to an unrealistic behavior. In the last few years have been proposed extended CA models that are able to reproduce even more subtle effects, e.g., meta-stable states of highway traffic [8]. Unfortunately, the comparison of simulation results with empirical data on a microscopic level is not that satisfactory. As it was discussed in chapter 2, the existing models fail to reproduce the microscopic structure observed in measurements of real traffic ([110] and chapter 3). But particularly in highway traffic a correct representation of the microscopic details is necessary because they largely determine the stability of a traffic state and therefore also the collective behavior of the system.
This chapter presents a comparison of some of the most prominent cellular automata (CA) with empirical results (see chapter 3), as well as a discussion of their degree of realism and their limitations. In particular, simulations of the following models are compared: the CA model proposed by Nagel and Schreckenberg which is to date the most frequently used CA approach for traffic flow, the VDR model [8] which is a realization of so-called slow-to-start models, the TOCA-model of Brilon *et al.* [13], the model of Emmerich *et al.* which uses velocity-gap matrices [28], and the approach by Helbing and Schreckenberg [47] which represents a model with a more sophisticated distance rule. Finally, based on the cellular automaton model of Nagel and Schreckenberg, an improved discrete model incorporating anticipation effects, reduced acceleration capabilities and an enhanced interaction horizon for braking is proposed. This modified model tries to capture the human driving behavior in the various traffic states that was discussed in the previous chapter.
The different models are compared with respect to their ability to reproduce the empirical situation. This implies that the measurement procedure is reenacted during the simulations. Analogously to empirical setups, the simulation data are evaluated by a virtual inductive loop, i.e., the speed- and the time-headway of the vehicles are measured at a given link of the lattice. The measurement process is applied after the update of the velocity has been carried out but right before the movement of the vehicles. This implies that the gap to the preceding vehicle does not change significantly during the measurement. These simulation data are analyzed taking individual and aggregated quantities into account, as it has been done in the empirical investigations of [110, 133] and in chapter 3. Although most of the empirical data sets have been collected at multi-lane highways, the simulations are performed on a single-lane road in order to reduce the number of adjustable parameters. This approach is justified because the empirical data sets are selected, so that

multi-lane effects are of minor importance.
Before the analysis of the above mentioned CA models, an empirical test scenario is introduced. The empirical results have been chosen with respect to their reproducibility and the ability to distinguish between the different traffic states. This scenario will be discussed in the next section.

4.1 Empirical facts

In order to probe the accuracy and the degree of realism of the different models, one has to introduce a test scenario that includes the most important empirical findings. The difficulty in defining such a scenario is due to the fact that the empirical results may depend strongly on the particular environment. Therefore one has to try to extract the results that really characterize the behavior of the vehicles. An additional difficulty results from the fact that mostly aggregated data have been analyzed which are known to be largely dependent on the road conditions, e.g., the capacity of an upstream bottleneck. A number of results, however, is of general nature as it will be discussed below.
Even more conclusive are the empirical investigations that use single-vehicle data. These results can be directly compared to the simulation results and include important information concerning the microscopic structure of vehicular traffic. Unfortunately, only a small number of empirical investigations that are based on single-vehicle data exists so far. The discussion refers to the empirical studies in chapter 3 and of refs. [110, 133]. In particular, in order to reduce the effects of disorder (the data sets analyzed in chapter 3 are taken from measurements of highways without speed limit), the results of [110] (except for the time-headway distributions, see below) are used for the comparison with simulation data. The empirical results that are taken as a basis for the comparison with the model results have been obtained from inductive loops. Measurements by inductive loops that represent the most frequently used measurement devices provide information about the number of cars passing, their velocities and the occupation times. These direct measurements are also used in order to calculate other quantities, e.g., the spatial distance d_n via equation (2.5).

4.1.1 Temporally aggregated data

The most important empirical quantity is the relation between the averaged quantities flow J and density ρ, i.e., the fundamental diagram. The results for the fundamental diagram are discussed in the different traffic phases and are based on one-minute data. The spatial density $\rho(t)$ can be calculated from the hydrodynamical relation [110] equation (2.6).
Free flow traffic is characterized by the high mean-value of the average speed. One basically observes two qualitatively different functional forms of the fundamental diagram, i.e., that the linear regime extends up to the observed maximum of the flow or that one has a finite curvature in particular for densities slightly below the density of maximum flow (Fig. 4.1). The finite curvature is a consequence of an alignment of speeds, i.e., close to the optimal flow it is not longer possible to drive systematically faster than the trucks. This point of view is supported by the empirical results taken from highways where a quite restrictive speed limit that can be reached even by trucks is applied. In this case the whole free flow branch is linear. In order to allow the comparison with simulation data, the linear form of the fundamental diagram is relevant because a single type of cars is used in the simulations, with a maximal velocity given by the slope of the free flow branch. When simulating a section of the highway where no speed limit is applied, one

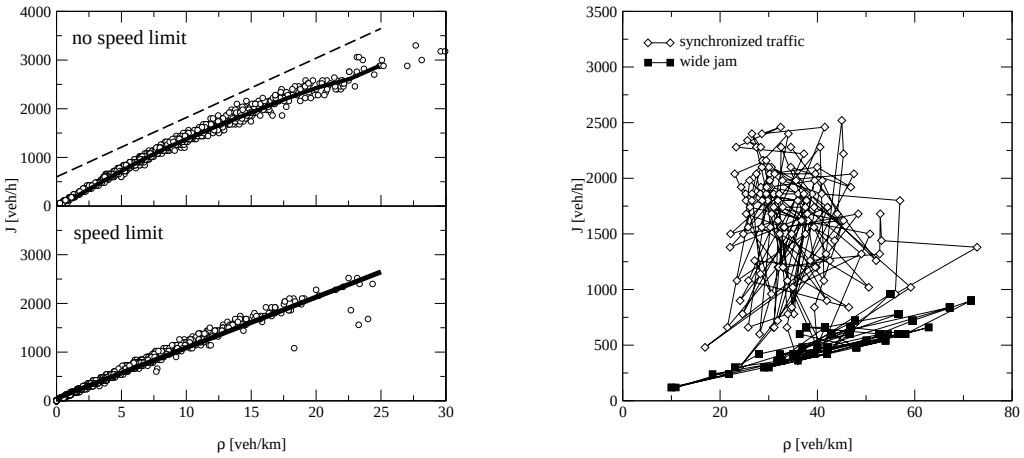

Figure 4.1: Left: Two empirical free flow branches at parts of the highway with (from the A3 data set of chapter 3) and without (from [109]) speed limits. The application of a speed limit leads to a reduced curvature of the free flow branch. Right: Time-traced fundamental diagram of the two congested states (from [109]). Synchronized traffic is characterized by strong fluctuations of the density and flow. The measurements for wide jams are similar to measurements in free flow but with much smaller average velocity.

has to take a distribution of maximal speeds. This distribution can be obtained from the empirical velocity distributions at very low densities, where interactions between cars can be neglected.
In the congested regime one distinguishes between synchronized traffic and wide jams. In the synchronized phase, the mean velocity of the vehicles is reduced, compared to the free flow, but the flow can take on values close to the maximum flow. Moreover, strong correlations between the density on different lanes exist caused by lane changings. The synchronized state has been subdivided into three types, which differ in the characteristics of the time series of density and flow (see section 2.2.1). In this chapter only synchronized flow of type 3 is considered, because the two other types of synchronized traffic have been rarely observed and it is not confirmed whether they are generic phases of traffic flow. An identification of synchronized traffic by means of the fundamental diagram may be misleading, because the results often depend on the averaging procedure. A more sensitive check is to identify the different types of traffic states by means of the cross-correlation $cc(J,\rho)$ of the density ρ and the flow J [110]:

$$cc(J,\rho) = \frac{\langle J(t)\rho(t)\rangle - \langle J(t)\rangle\langle\rho(t)\rangle}{\sqrt{\langle J^2(t)\rangle - \langle J(t)\rangle^2}\sqrt{\langle\rho^2(t)\rangle - \langle\rho(t)\rangle^2}}. \tag{4.1}$$

The linear dependency of the flow and the density in the free flow state as well as in the wide jam state leads to cross-correlations of ≈ 1, whereas irregular patterns of the flow and the density in the synchronized traffic of type 3 lead to cross-correlations of ≈ 0.
Fig. 4.1 includes typical measurements of the fundamental diagram that correspond to wide jams. Surprisingly, these measurements reveal quite small values of the density,

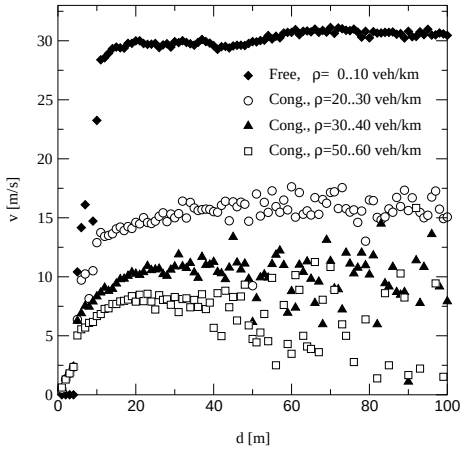

Figure 4.2: Empirical optimal-velocity (OV) functions, i.e., speed-distance relations. The figure shows the mean velocity for a given spatial distance and different traffic states. From [110].

although the road is almost completely covered by cars. This seemingly incorrect result is due to the local nature of the measurement (see [110] for a detailed discussion). Thus, the form of the fundamental diagram in the jammed state is similar to free flow traffic, but with a small average velocity.

4.1.2 Single vehicle data

Similar to the time-averaged observables, the results for the microscopic quantities differ qualitatively in the different phases.
The first quantity that is looked at is the time-headway distribution, i.e., the time elapsing between two cars passing the detector [1]. This quantity is the microscopic analogue to the inverse flow. In free flow traffic, one has found that the distribution at short times as well as the position of the maximum is independent of the density (cf. Fig. 3.6).
The *cut-off* at small time-headways as well as the *typical* time-headway in free flow traffic are important observables that have to be reproduced by the microscopic models. The exact shape of the distribution may also depend on the relative frequency of slow vehicles, because this determines the fraction of interacting vehicles at a given density.
The time-headway distributions in synchronized traffic (cf. Fig. 3.9) differ systematically from the free flow distributions [2]. In synchronized traffic the distributions have a maximum that is much broader than that in free flow traffic. The maximum is less pronounced, and its position depends significantly on the density.

[1] In this chapter the simulation data is compared with the results of the analysis of empirical single-vehicle data of [109, 110]. However, since the time-headway distribution in free flow as well as in the synchronized state shows some peculiarities due to an error of the measurement software, the distribution in the free flow regime is calculated from new measurements on the A1 (cf. section 3.2).

[2] Unfortunately, new measurements taken from the A1 do not provide a sufficient amount of data of the synchronized state. Since the time-headway distributions of [109, 110] cannot be used, the distribution is calculated from data sets taken from the A3 (cf. section 3.3). This is justified because the effects of a speed limit can be neglected at larger densities.

In the presence of wide jams one has to distinguish between the jam and the outflow region of a jam. In the jam one finds evidently a broad distribution of time-headways, because cars are blocked for quite long times. In the outflow region of a jam, however, one observes that the typical time headway is of the order ~ 2 s.
The characteristics of traffic jams also belong to the extensively studied phenomena in traffic flow. Wide traffic jams can be identified by a sharp drop of the velocity and the flow to negligible values in the time-series. Moreover, traffic jams move upstream with a surprisingly constant velocity (typically 15 km/h [67]) that does not change as far as the the control parameters of traffic, like the weather or the road conditions do not change. The upstream velocity is intimately related with the outflow from a jam J_{out} that also takes on constant values for a given situation. This allows the observed coexistence of jams. The coexistence is facilitated because the outflow from a jam is considerably smaller than the maximal flow $J_{\max}$, so that no new jams emerge in the outflow region of a jam. In empirical analyses one has observed the ratio $J_{\max}/J_{\text{out}} \approx 1.5$. The outflow and the upstream velocity of a jam can therefore also be used in order to calibrate the model. The precise data for the average upstream velocities and J_{out} may also serve in order to evaluate the average space Δs that is occupied by a car in a jam. Often, the length of a cell in the CA models is represented by Δs and not by the average length of the vehicles. Δs may also be used to assign a reasonable value of the velocity of cars in a jam, i.e., $v_n = \Delta s / t_n^h$.
The final test of the models results from the velocity distance relation in the different traffic phases (Fig. 4.2). These relations characterize in great detail the microscopic structure of the different phases. Some models use the velocity-distance or "optimal velocity" curve directly as an input [5] (see section 2.6.2). In any case, this quantity is a sensitive test concerning the reproduction of the microscopic structure of highway traffic. In the free flow regime, the asymptotic velocity is reached for small headways. The asymptotic velocity does not depend on the density but is given by the applied speed limit. In the congested regime this asymptotic velocity is much smaller than in free flow, i.e., cars are driving slower than the distance-headway allows. Therefore, the asymptotic velocity does not only depend on the density but also on the traffic state. But also at short distances one obtains different functional forms for different densities. This observation reflects the important differences between free flow and synchronized traffic in the microscopic structure of both states.

4.2 Simple stochastic CA models

Throughout this chapter are investigated microscopic traffic models that are discrete in time and space. The discreteness of the models has the advantage that they can be directly and very efficiently used for computer simulations, in particular without any further discretization errors. The discreteness of the model, however, also leads to some difficulties, particularly when describing congested traffic. E.g., in congested traffic, a continuous range of typical velocities exists that depend strongly on the density. This velocity interval is mapped on a discrete set of velocity variables. So even for an optimal reproduction of the traffic state, an upper limit for the accuracy of the models exists.
Moreover, the temporal discretization introduces a characteristic time-scale. This time-scale can be understood, if a parallel update is applied, as the effective reaction-time of the drivers that is explicitly included in car-following models. Furthermore, the temporal discretization becomes obvious as peaks in the measurement of the time-headways t_n^h. The finer the discretization, the less pronounced the peaks. Nevertheless, one has to find

a compromise between realism and complexity. In order to increase the resolution, the time-headways in the simulations are calculated via the relation $t_n^h = \frac{d_n}{v_n}$. The minimal resolution, however, is restricted by the discretization that determines the minimal difference of the time-headways $\frac{l}{v_{\max}}$ in free flow with the length l and the maximum velocity $v_{\max}$ of a vehicle. In order to facilitate a comparison with empirical time-headways, the distributions are normalized via $\sum P(t^h) \cdot \Delta t^h = 1$.
A number of traffic models is discussed below in detail with respect to their agreement with the empirical findings of the test scenario. Beyond that it is demanded that each model reproduces some basic phenomena like the spontaneous jam formation and fulfills minimal conditions as, e.g., being free of collisions. These conditions are generally understood as fulfilled if the opposite is not explicitly stated. In particular, deterministic models that lack the ability of the spontaneous formation of jams [32] which is a result of the inherent stochasticity of traffic flow rather than a consequence of perturbations that are not a subject of this study.
The simulations are performed on a periodic single-lane system. This simple structure of the system is in sharp contrast with realistic highway networks. It is nevertheless justified, because it has been shown for a large class of models, that different boundary conditions select different steady states rather than change their microscopic structure. Also the restriction to single-lane traffic is of minor importance for the empirical test scenario, which has been discussed in the previous section.
It has also to be mentioned that a single set of parameters is chosen for each model. Some of the model parameters can be directly related to a given empirical quantity. In this case, the value is chosen that leads to an optimal agreement with the related observable. In this way it is avoided to rank the importance of the empirical findings.
For a particular application of the model, however, the reproduction of a certain quantity might be of special interest, and therefore a calibration of the model that differs from the one used here is more appropriate.

4.2.1 The CA model of Nagel and Schreckenberg

The microscopic model introduced by Nagel and Schreckenberg [106] (hereafter cited as "NaSch model") is the prototype of microscopic models that is discussed in this chapter. The important role of this model is mainly due to its simplicity that allows very fast implementations. In fact, the NaSch model is a minimal model, in the sense that every simplification leads to a loss of realism. The model is also used as a reference for other models that will be introduced by indicating the relation to the NaSch model.
For the sake of completeness, the definition of the NaSch model although given in section 2.6.4 is briefly summarized. The NaSch model is a discrete model for traffic flow. The road is divided into cells that can be either empty or occupied by car n with a velocity $v_n = 0, 1, ..., v_{\max}$. Cars move from the left to the right on a lane with periodic boundary conditions, and the system update is performed in parallel according the four following rules:

1. Acceleration: $v_n\left(t + \frac{1}{3}\right) = \min\left(v_n(t) + 1, v_{\max}\right)$
2. Deceleration: $v_n\left(t + \frac{2}{3}\right) = \min\left(v_n\left(t + \frac{1}{3}\right), d_n\right)$
3. Noise: $v_n(t+1) = \max\left(v_n\left(t + \frac{2}{3}\right) - 1, 0\right)$ with probability p_{dec}
4. Motion: $x_n(t+1) = x_n(t) + v_n(t+1)$

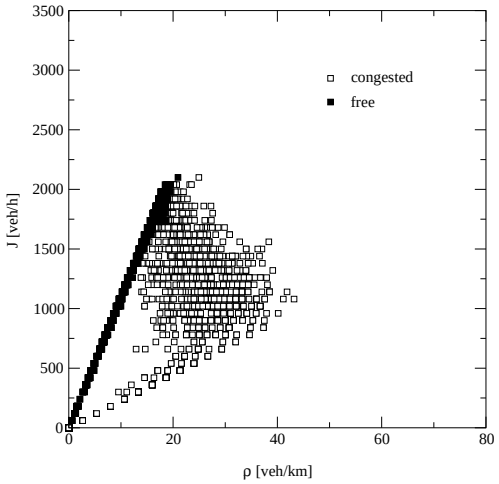

Figure 4.3: Local fundamental diagram of the NaSch model for $v_{\max} = 112$ km/h = 5 cells/δt, time-step $\delta t = 1.2$ s and $p_{\text{dec}} = 0.16$. A cell has a length of 7.5 m.

with the velocity v_n, the maximum velocity $v_{\max}$ and the position x_n of car n. d_n specifies the number of empty cells in front of a car.
For a given discretization, the model can be tuned simply by varying the two parameters $v_{\max}$ and p_{dec}. The value of $v_{\max}$ mainly affects the slope of the fundamental diagram in the free flow regime, while the behavior in the congested regime is controlled by the braking noise p_{dec}. Each time step corresponds to 1.2 s in reality, and the length of a cell is given by 7.5 m. The length of a cell corresponds to the average space occupied by a vehicle in a jam, i.e., its length and the distance to the next vehicle ahead. This choice is in accordance with measurements at German highways on the left and middle lane, where the density of trucks is low [63]. Due to the parallel update, an implicit reaction time is introduced, and the value has to be chosen accordingly. Please note that this time is not the reaction time of the driver (that would be much shorter) but the time between the stimulus and the actual reaction of the vehicle. The value that is chosen allows to reproduce the typical upstream velocity of a jam.
The two free parameters of the model are tuned by adjusting the slope in the free flow regime and the maximum of the fundamental diagram. Fig. 4.3 shows the resulting fundamental diagram using $v_{\max} = 112$ km/h = 5 cells/time-step and $p_{\text{dec}} = 0.16$ that has to be compared with the empirical results.
By tuning the parameters, the free flow branch of the fundamental diagram could be reproduced quite well: Both, the slope as well as the maximum are in agreement with the empirical findings. For congested traffic, however, the model fails to reproduce the two distinct phases, in particular the characteristics of synchronized traffic are not matched. This interpretation of the flow data is supported by measurements of the cross-correlation function that is negative in the corresponding density regime. In the presence of wide jams, the flow is proportional to the densities as found by empirical observations. But also for wide jams exist differences. In real measurements, the branch extends up to quite high densities (~ 70 veh/km), while the simulation results are restricted to lower densities (~ 40 veh/km).

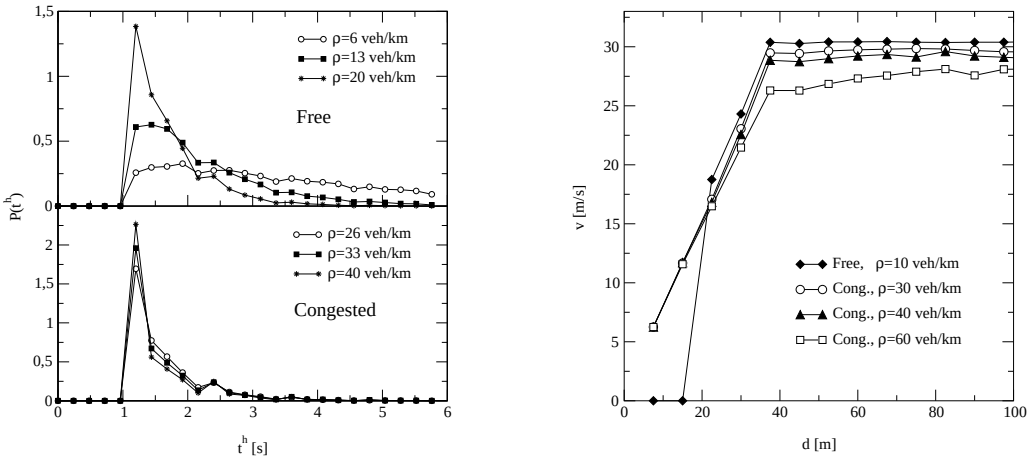

Figure 4.4: Time-headway distribution (left) and OV-function (right) of the NaSch model in free flow and congested traffic for different densities.

In the following, the model is discussed on a microscopic level. As mentioned above, the upstream velocity of wide jams can be tuned by choosing the appropriate discretization δt of the time. The calibration has been verified by initializing the system by a large jam and measuring the velocity of the upstream propagation of the jam front. As expected, the result is in agreement with the empirical data. Nevertheless, the dynamics of jams in the NaSch model is in contradiction to the empirical findings because emergent jams are observed in the outflow region of a jam. This implies that the observed parallel propagation of jams cannot be reproduced by the NaSch model.
The time-headway distributions of the NaSch model also mismatch with the empirical results (Fig. 4.4). Due to the discreteness of the model and the unique maximal velocity of the cars, the distribution function has a peaked structure. But more important than that is the absence of time-headways shorter than the chosen unit of time. This implies that the cut-off at short times and the upstream velocity of jams cannot be reproduced at the same time.
Finally, also the optimal velocity curves of the model (Fig. 4.4) are discussed. In congested traffic one observes only a very weak dependence of the "optimal velocity" on the density. This is due to the short range of interactions in the model and the strong acceleration of the cars. So neither a significant density dependence nor a sensitivity to the traffic state is observed. Both findings are serious contradictions to the empirical findings, expressing a faulty description of the microscopic structure of the model.

4.2.2 The VDR model

A first step towards a more realistic model of traffic flow was made by the so-called velocity-dependent-randomization (VDR) model [8, 127, 132] that extends slightly the set of update rules of the NaSch model. In this model, a velocity-dependent randomization $p_{\mathrm{dec}}(v)$ is introduced that is calculated before application of step 1 of the NaSch model.

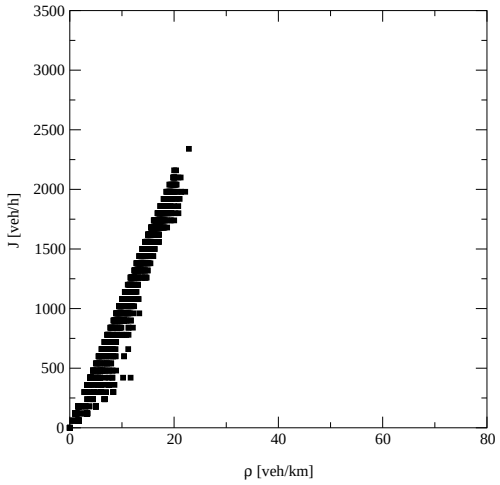

Figure 4.5: Local fundamental diagram of the VDR model for $v_{\max} = 108$ km/h = 3 cells/δt, time-step $\delta t = 0.75$ s, $p_0 = 0.58$ and $p = 0.16$.

As a simplest version of VDR, a different p_{dec} for cars with $v = 0$ was studied:

$$p_{\text{dec}}(v) = \begin{cases} p_0, & v = 0 \\ p, & v > 0 \end{cases} \tag{4.2}$$

with $p_0 > p$.
The additional rule of the VDR model has been introduced in order to reproduce hysteresis effects. This is indeed possible because the new parameter p_0 allows to tune the velocity and the outflow of wide jams separately. As a side effect, it is now possible to keep the unit of time small and to reproduce the empirical observed downstream velocity of jams. The parameters of the model were chosen in the following way: The unit of time is adjusted in order to match the position of the maximum of the time-headway distribution. Then the parameter p_0 is chosen such that the measurements of the upstream velocity of a jam could be reproduced. Finally, $v_{\max}$ and p ensure a good agreement in the free flow branch. Fig. 4.5 shows the fundamental diagram of the VDR model. Obviously, the model fails to reproduce the congested phase correctly. Compared to the NaSch model the mismatch of the fundamental diagram in the congested regime is even more serious, i.e., it is not possible at all to identify a density regime as synchronized traffic. The reason for this can be found in a stronger separation between free flow and wide jams. This separation reduces the weight of the measurements that interfere between wide jams and free flow. Results comparable to the NaSch model could be obtained close to a perturbation, e.g., a bottleneck, where the typical size of jams is still short [1, 7], and accelerating and braking cars have a larger weight.
But in any case, this way of generating synchronized states by the boundary conditions does not agree with the empirical situation because one cannot reproduce the large spatial and temporal extension of the synchronized state. The missing synchronized traffic phase leads to quite large positive values of the cross-correlation $cc(J, \rho)$ of the density and the flow.
The time headway distribution of the VDR model differs in two points from the empirical observations (Fig. 4.6). (i) The unit of time is a sharp cut-off, i.e., the short time charac-

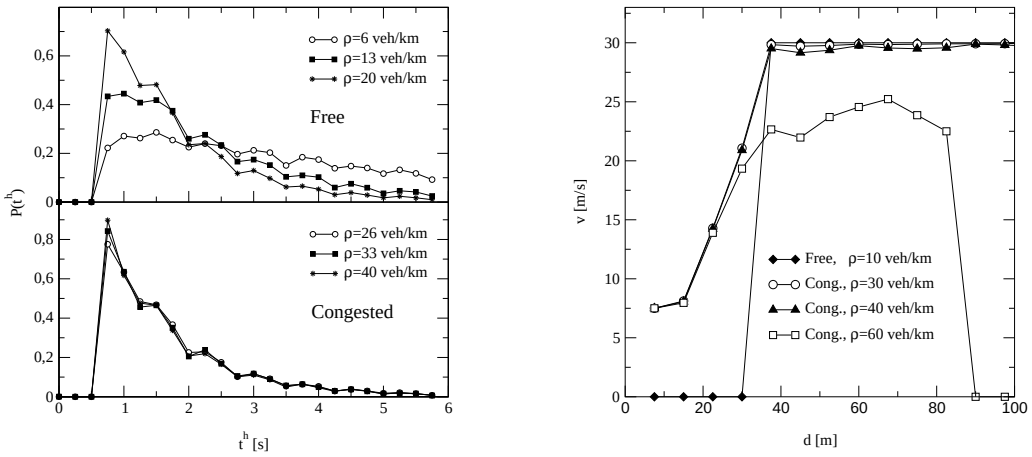

Figure 4.6: Time-headway distribution (left) and OV-function (right) of the VDR model in free flow and congested traffic for different densities.

teristics of the time headway distribution is not in agreement with the empirical findings. (ii) A density dependence of the maximum in congested traffic cannot be observed. Similar results are obtained for the OV-functions that do not depend on the density or the traffic state (Fig. 4.6). This fact is a consequence of the microscopic structure of high density states. At large densities, compact wide jams and zones of free flow traffic coexist, separated by a narrow transition layer. Now, the virtual "detector" measures only moving cars and therefore almost freely moving cars even at large densities.
The major achievement of the VDR model is the correct description of the dynamics of wide jams. The outflow from a jam is lower than the maximal flow, and therefore jams do not emerge in the outflow region. This effect leads to the increased stability of jams, including the empirically observed parallel upstream motion of two jams.
The analysis of the VDR model showed even more clearly the effect of a missing synchronized traffic phase. While in the NaSch model the density can be chosen such that a scattered structure in the fundamental diagram appears, rather pure free flow states and wide jams for the VDR model are obtained. Contrary, the VDR model gives a much better description of the dynamics of jams.

4.2.3 The TOCA model

Based on the CA model of Nagel and Schreckenberg, Brilon *et al.* [13] proposed a time oriented CA model (hereafter cited as TOCA) that increases the interaction horizon of the NaSch model (in the NaSch model cars interact only if $d \leq v$) and therefore changes the car following behavior.
Compared to the NaSch model, the acceleration step is modified, i.e., a car n accelerates only if its temporal headway $t_n^h = d_n/v_n$ is larger than some safe time headway t^s. But even for sufficiently large headways the acceleration of a vehicle is not deterministic but is applied with probability p_{ac}. As a second modification, also the randomization step is modified, i.e., it is applied only for cars moving with short time-headways ($t^h < t^s$). The limited interaction radius of this third step leads, for a given value of p_{dec}, to a reduction

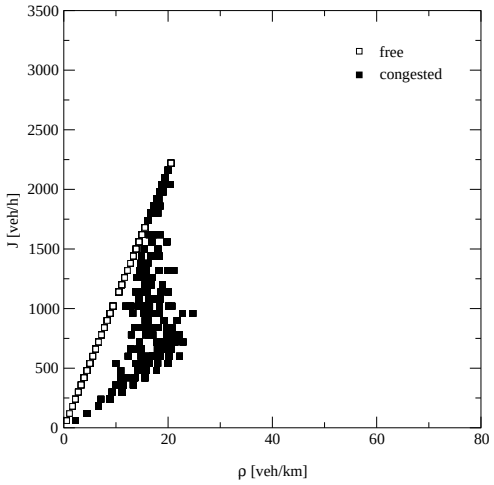

Figure 4.7: Fundamental diagram of the TOCA model. The following discretization is used: Length of a cell 7.5 m. Each time-step corresponds to $\delta t = 1$ s in reality. The parameters of the model are set to the following values $t^s = 1.2$, $p_{\mathrm{ac}} = 0.9$ and $p_{\mathrm{dec}} = 0.9$, $v_{\max} = 4$ cells/δt $= 108$ km/h.

of the spontaneous jam formation.
The update rules then read as following:

1. if$(t_n^h > t^s)$ then
   $v_n\left(t + \frac{1}{3}\right) = \min\left(v_n(t) + 1, v_{\max}\right)$ with probability p_{ac}
2. $v_n\left(t + \frac{2}{3}\right) = \min\left(v_n\left(t + \frac{1}{3}\right), d_n\right)$
3. if$(t^h < t^s)$ then
   $v_n(t+1) = \max\left(v_n\left(t + \frac{2}{3}\right) - 1, 0\right)$ with probability p_{dec}
4. $x_n(t+1) = x_n(t) + v_n(t+1)$

with $t^s = 1.2$, $p_{\mathrm{ac}} = 0.9$ and $p_{\mathrm{dec}} = 0.9$ [13]. For the comparison with the NaSch and VDR model, $v_{\max} = 4$ is used. With this choice of t^s, the update rules can be simplified for $v_{\max} \leq 4$, because of the discrete nature of the model:

1. $v_n\left(t + \frac{1}{3}\right) = \min\left(v_n(t) + 1, v_{\max}\right)$ with probability p_{ac}
2. $v_n\left(t + \frac{2}{3}\right) = \min\left(v_n\left(t + \frac{1}{3}\right), d_n\right)$
3. $if\ \left(d_n \leq v_n\left(t + \frac{2}{3}\right)\right)$ then
   $v_n\left(t+1\right) = \max\left(v_n\left(t + \frac{2}{3}\right) - 1, 0\right)$ with probability p_{dec}
4. $x_n(t+1) = x_n(t) + v_n(t+1)$.

As expected for this parameterization of the model, results for the fundamental diagram are obtained that are comparable to the NaSch model (Fig. 4.7). In comparison with the empirical data, the values of the density in congested traffic are too small, the upper limit is even shifted towards smaller values.

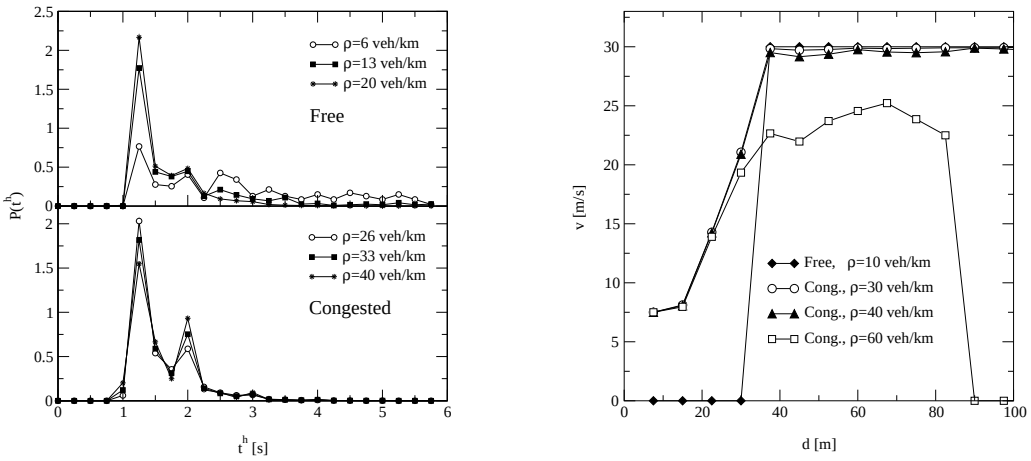

Figure 4.8: Time-headway distribution (left) and OV-function (right) for the TOCA model in free flow and congested traffic for different densities.

The time-headway distributions of the TOCA model, however, differ significantly from the results of the NaSch model (Fig. 4.8). For free flow traffic, the position of the maximum differs from the minimal time-headway. The maximum coincides for the chosen set of parameters with t^s, while the minimal time-headway is determined by the chosen unit of time. For congested traffic, the distribution has two maxima, one corresponding to the typical time-headway in free flow traffic, and the other corresponding to the typical temporal distance in the outflow region of a jam.
The OV-function of the TOCA and the NaSch model differ in two respects (Fig. 4.8). (*i*) Due to the fact that the randomization step is applied for a finite range of the interactions, all cars move deterministically with $v_{\max}$ at low densities, and therefore spatial headways smaller than v_{max} cells are completely avoided. This result is at least partly a consequence of the simulation setup, i.e., choosing exactly the same maximal velocity for every car. (*ii*) The second difference lies in the density dependence of the OV-function for congested traffic. Because of the retarded acceleration in step 1 and the deceleration of vehicles with $v \leq d$, at very large densities the system contains only one large jam with a width comparable to the system size. As a consequence, the mean velocity at a given distance is reduced considerably compared to free flow. The transition to a completely jammed system occurs at densities of about 66 veh/km and leads to the abrupt change of the OV-curve.
The main difference between the NaSch model and the TOCA approach lies in the structure of jams. Due to the restricted application of the randomization step, p_{dec} must be quite large in order to obtain reasonable results for the fundamental diagram. This choice of p_{dec}, however, reduces significantly the density of jams. This implies that, although the typical time-headway in the outflow region of a jam has the correct value, the downstream velocity of jams is too large.
The analysis revealed several shortcomings of the TOCA model. However, the TOCA model is an interesting advancement of the NaSch model if a finer discretization is applied. This can be illustrated for the example of the density of a wide jam: The inverse density

of wide jams was used in order to fix the size of a cell. This choice is correct, as the jams in the model are basically compact, which is not true in case of the TOCA model. In this case more accurate results could be obtained if each cell would be divided into three cells. Using this finer discretization, cars would occupy two cells which would finally lead to a quite realistic dynamics of jams. A more elaborate discussion of discretization effects can be found in appendix B.

4.3 CA models with modified distance rules

4.3.1 The model of Emmerich & Rank

The CA model introduced by Emmerich & Rank [28] (ER-model) is another variant of the NaSch model with an enhanced interaction radius. Precisely speaking, the braking rule of the NaSch model is replaced by applying a velocity dependent safety rule that is implemented via a gap-velocity matrix M. The entries $M_{i,j}$ of M denote the allowed velocities for a car with a gap i and velocity j. Replacing the braking rule $M_{ij} \leq j$ holds because otherwise the car would accelerate. For the NaSch model the gap-velocity matrix simply reads $M_{i,j} = \min(i, j)$.
In order to increase the interaction horizon, Emmerich and Rank enlarged this matrix, so that even for a gap of 9 cells the maximum velocity is restricted to 4. In their model M is given as:

$$M_{ER} = \begin{pmatrix} 0 & 0 & 0 & 0 & 0 & 0 \\ 0 & 1 & 1 & 1 & 1 & 1 \\ 0 & 1 & 2 & 2 & 2 & 2 \\ 0 & 1 & 2 & 3 & 3 & 3 \\ 0 & 1 & 2 & 3 & 4 & 4 \\ 0 & 1 & 2 & 3 & 4 & 4 \\ 0 & 1 & 2 & 3 & 4 & 4 \\ 0 & 1 & 2 & 3 & 4 & 4 \\ 0 & 1 & 2 & 3 & 4 & 4 \\ 0 & 1 & 2 & 3 & 4 & 4 \\ 0 & 1 & 2 & 3 & 4 & 5 \end{pmatrix}$$

for $v_{\max} = 5$ and $d \leq 10$.
As a second modification of the NaSch model, a different update scheme is applied. The ER model uses an ordered sequential update scheme, i.e., all rules, including the movement of the vehicles, are directly applied for the chosen car. A unit of time is elapsed after updating all cars. Ordered sequential updates use normally a fixed sequence of cars or lattice sites. This leads to the disadvantage that some observables, e.g., the typical headway, may depend on the position of the detection device, even for periodic systems. In order to reduce this effect, first the car with the largest gap is chosen, than the update propagates against the driving direction.
As a consequence of the ordered sequential update scheme, the gaps are used very efficiently, and very high flows can be achieved [119]. (Now, it is allowed that two cars are driving with $v_{\max}$ and $d = 0$, so that flows $J > 1$ veh/δt are possible). Therefore large deceleration probabilities are necessary to decrease the overall flow to realistic values. Furthermore, due to the sequential update scheme, the spontaneous jam formation is reduced considerably. The application of a sequential update is crucial. If this update scheme is replaced, e.g., by a parallel update, one may observe an unrealistic form, i.e., a

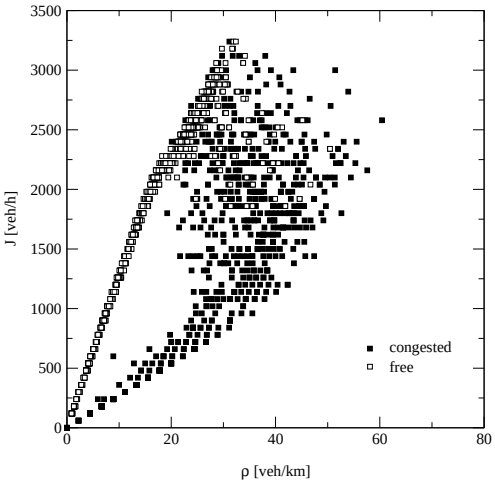

Figure 4.9: Fundamental diagram of the ER-model. As suggested in the original work a cell length of 7.5 m, $\delta t = 1$ s, $p_{\mathrm{dec}} = 0.3$ and $v_{\mathrm{max}} = 5$ cells/time-step = 135 km/h is chosen.

non-monotonous behavior, of the fundamental diagram at low densities.
As a consequence of the special choice of M, the velocity of cars with $d \leq 9$ is restricted to $v \leq 4$. This means that a generic speed limit with $v_{max} = 4$ is applied for all densities $\rho \geq 1/11 = 12$ veh/km, where the mean distance between the cars is smaller than 10 cells. Therefore, the free flow branch of the fundamental diagram in Fig 4.9 has, in contrast to the empirical data, two different slopes, one corresponding to $v_{\mathrm{max}} = 5$ cells/δt if $\rho < 15$ veh/km and the other to $v_{\mathrm{max}} = 5$ cells/δt at larger densities.
For the present choice of M, the distance rule of the NaSch model with $v_{\mathrm{max}} = 4$ cells/δt is basically recovered because the speed limit applies only for larger distances. Therefore, the structure of the congested part of the fundamental diagram, is quite similar to the NaSch model.
Although the results of the fundamental diagram of the ER-model are comparable to the NaSch model, important differences concerning the microscopic structure of the traffic state exist. These differences are due to the modified update scheme. By applying an ordered sequential update, it is possible to drive with high speed and small distances. This could in principle (for small p_{dec}) lead to very short time headways. For the chosen value of p_{dec}, however, the typical time-headways are quite large in the free flow regime and do not match the empirical findings. Nevertheless, the ordered sequential update changes qualitatively the form of the time-headway distribution, i.e., the position of the maximum and the short time cut-off are different, as empirically observed (Fig. 4.10).
The OV-function of the ER-model differs strongly from the empirical findings (Fig. 4.10). For this quantity, the modified distance rule is of great importance. In the congested regime, plateaus of almost constant average velocities $v < v_{\mathrm{max}}$ can be observed. The density dependence of the OV-function is, as for the NaSch model, very weak. In free flow traffic, small headways simply have not been observed, in contradiction to the empirical results.
The most important weakness of the ER-model is its description of the jam dynamics.

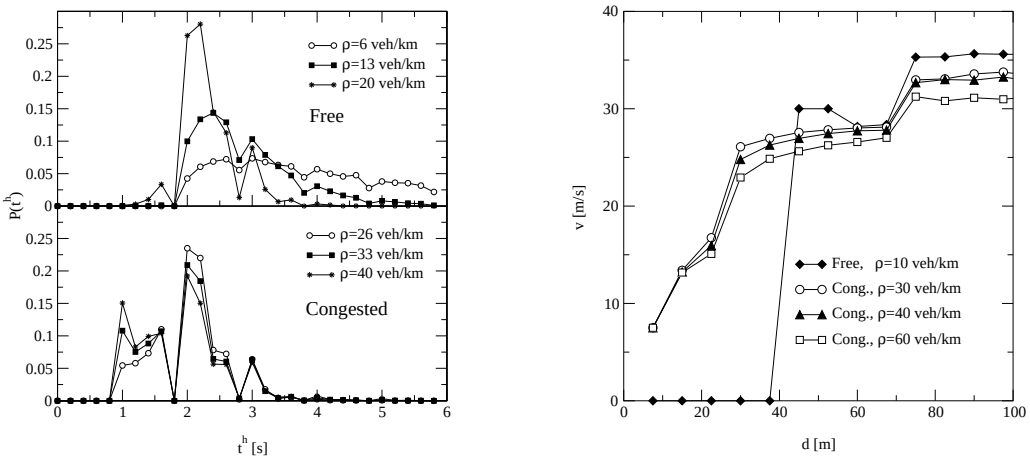

Figure 4.10: Time-headway distribution (left) and OV-function (right) for the ER model in free flow and congested traffic for different densities.

First of all, for small values of p_{dec}, the possibility of downstream moving jams exist, which contradicts all empirical studies. But even for the large value of p_{dec} that was applied, jams are not stable, i.e., often branch into a number of small jams. Therefore it is impossible to reproduce the empirically observed parallel moving jams with the ER-model. In summary, the gap-velocity matrix allows on one hand a more detailed modeling of the interaction horizon. On the other hand, the sequential update leads to a very unrealistic structure of the microscopic traffic states.

4.3.2 A discrete optimal velocity model

Helbing and Schreckenberg (HS) [47] have introduced a cellular automaton model for the description of highway traffic based on the discretization of the optimal-velocity (OV) model of Bando et al. [5].
The deterministic part of the velocity update is done by assigning the following velocity to the cars:

$$v_n(t+1) = v_n(t) + \Big\lfloor \lambda[V_{\mathrm{opt}}(d_n) - v_n(t)] \Big\rfloor \tag{4.3}$$

where $V_{\mathrm{opt}}(d)$ denotes the "optimal" velocity of car n for a given distance d_n to the vehicle ahead, $v_n(t)$ the discrete velocity at time t and $\lfloor \ldots \rfloor$ the floor function. The constant λ is a free parameter of the model. The deterministic update is followed by a randomization step as known from the NaSch model, i.e., the velocity of a car with $v_n(t+1) > 0$ is reduced with probability p_{dec} by one unit. [3] The acceleration step is the naive discretization of the acceleration step of the space and time continuous OV model. In the continuous version of the OV model, the parameter λ determines the timescale of the acceleration. However, for time-discrete models it is well known that a simple rescaling of time is not possible. Therefore the meaning of the parameter λ remains unclear.

[3] In contrast to the original work, here, only the case of one type of cars is considered and the index $a = 1$ is omitted on all quantities. Furthermore the OV function is denoted by V_{opt} so that it can be better distinguished from the velocities of the cars.

Although the model seems to be quite similar to the models discussed in the previous sections, important differences exist. In all other models discussed so far acceleration is limited to one velocity unit per time-step while breaking from $v_{\max}$ to zero velocity is possible. This is not true for the HS model where a standing car may accelerate towards $\lfloor \lambda V_{opt}(\infty) \rfloor$ in a single time-step. On the other hand, in particular for small values of λ, the braking capacity of cars is reduced. A reduced braking capacity, however, may lead to accidents (see the discussion in [85]), a certainly unwanted feature of a traffic model.
The possibility of accidents is now discussed in some more detail. In order to ensure that the model is free of collisions with *a*ny possible initial condition, the condition

$$v_n(t+1) \leq d_n(t) - 1 + v_{n+1}(t+1) \tag{4.4}$$

must always be fulfilled, i.e., the new velocity $v_n(t+1)$ of a car has to be smaller than the number $d_n - 1$ of empty cells in front plus the number $v_{n+1}(t+1)$ of cells the preceding car moves in the next time-step. Equation (4.4) has to be complemented by the inequality, $0 \leq v_n(t+1)$ which ensures that vehicles do not move backwards.
Consider now the case where the vehicle approaches the end of a jam, i.e., the preceding car is standing and will not move in the next time-step ($v_{n+1}(t+1) = 0$). Using the acceleration rule equation (4.3) condition equation (4.4) can be rewritten as

$$v_n(t+1) + \left\lfloor \lambda [V_{\text{opt}}(d) - v_n(t+1)] \right\rfloor \leq d_n - 1. \tag{4.5}$$

In order to be intrinsically free of collisions, condition (4.5) has to be satisfied for all d and all v. For $\lambda = 1$ the inequality (4.5) is always satisfied if $V_{\text{opt}}(d) \leq d_n - 1$. For general λ, however, this is not the case.
For the simulations the following OV-function is chosen:

d $[\Delta x]$	$V_{\text{opt}}(d)$ $[\Delta x/\delta t]$	d $[\Delta x]$	$V_{\text{opt}}(d)[\Delta x/\delta t]$
0, 1	0	11	9
2	1	12	10
3 – 5	2	13,14	11
6	3	15,16	12
7	4	17,18	13
8	5	19 – 23	14
9	6	24 – 37	15
10	7	≥ 38	16

Note that a vehicle cannot have a velocity of 8 cells due to the discretization of the OV-curve. The length of a cell is set to 2.5 m, $\delta t = 1$ is chosen as the unit of time and $\lambda = 0.77$. For this choice of the OV function the model is not free of collisions. This can easily be verified by initializing the system in a compact jam. In the simulations, jams *always* occurred for global densities larger than 20 veh/km when the first car arrived at the jam. This simulation result has to be discussed in the context of the empirical results of the jam dynamics. Empirically, one observes quite often a jam surrounded by free flow traffic. This includes the fact that cars approach the upstream front of jams with a rather large velocity. Unfortunately for the HS model, these kind of configurations lead to accidents, which is in sharp contrast to the real situation.
But how does one have to choose λ for a given OV function? Using the inequalities, $x \geq \lfloor x \rfloor > x - 1$ (for $x < 0$) one can derive sufficient conditions on the sensitivity parameter λ for the model to be *realistic* in the sense that no collisions occur

$$\lambda > \max \left\{ \frac{d - v - 1}{V_{opt}(d) - v} : v > V_{opt}(d) \right\}, \tag{4.6}$$

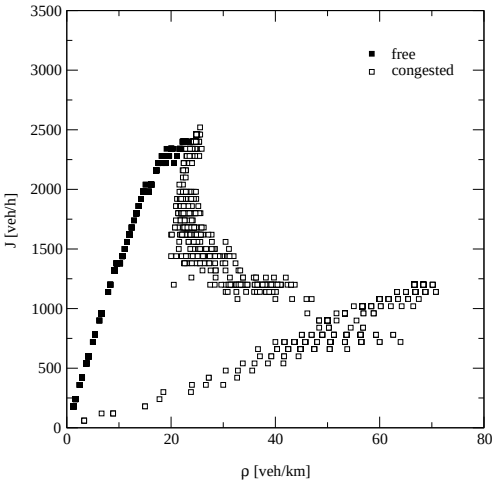

Figure 4.11: Fundamental diagram of the HS-model. As suggested in the original work the length of a cell is chosen to be 2.5 m, a vehicle has a length of 3 cells, $\delta t = 1$ s, $p_{\mathrm{dec}} = 0.001$, $v_{\max} = 16$ cells/time-step $= 144$ km/h and $\lambda = 1$.

and vehicles do not move backwards

$$\max\left\{\frac{d-v-1}{V_{\mathrm{opt}}(d)-v} : v > V_{\mathrm{opt}}(d)\right\}. \tag{4.7}$$

These two conditions have been checked for the OV-function given in [47]. It turns out that for the chosen V_{opt}-function $\lambda = 1$ is the only possible choice. The upper limit for λ holds for a quite general class of OV-function, i.e., it is the upper limit for all OV-functions having $V_{\mathrm{opt}} = 0$ for some value of the gap.
In order to provide a comparison with the models analyzed in the previous sections, simulations of the HS model are also performed. In particular, a cell length of 2.5 m, $\delta t = 1$ and a randomization probability $p_{\mathrm{dec}} = 0.001$ are used. λ is set to 1 in order to keep the model free of collisions. A vehicle has a length of $l = 3$ cells $= 7.5$ m.
The deterministic behavior of the model leads to speed limits in certain density regimes $l/(d_{\max}+l) < \rho < l/(d_{\min}+l)$ with $V_{\mathrm{opt}}(d_{\min}) = V_{\mathrm{opt}}(d_{\max})$ that become visible in different slopes in the free flow branch of the fundamental diagram. But also in the congested regime the rapid decrease of the OV-curve at intermediate headways results only in a small density regime that can be measured by the detector. However, since the OV-curve for vehicles at rest increases very slowly, the propagation of holes in large jams allows to detect larger densities than in the NaSch model (Fig. 4.11).
The main difficulties of the model in reproducing the empirical results become visible on a microscopic level. The model results of the time-headway distribution (Fig. 4.12) show a strong density dependence of the maximum of the distribution for the free flow states. This is due to the long-ranged interactions that tend to generate traffic states that are very homogeneous. Therefore short time-headways are suppressed at low densities. The second problem is the quasi-deterministic character of the model. This implies that drivers obey the distance rule in almost any case. As a result the peak values of the time-headway distribution have extremely large weights. In congested traffic a density independent position of the maximum of the time-headway distribution is observed. The

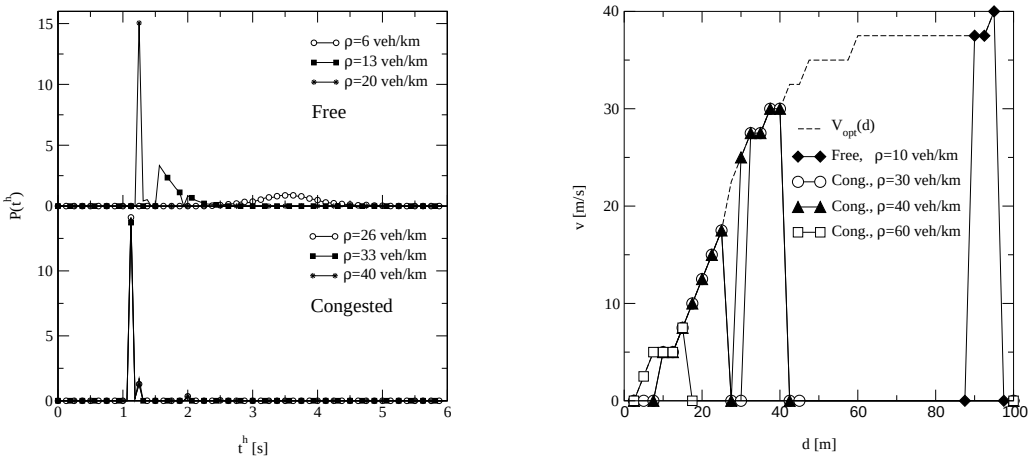

Figure 4.12: Time-headway distribution (left) and OV function (right) for the HS model in free flow and congested traffic for different densities.

maximum carries almost the whole weight of the distribution, in contradiction to the empirical findings.
The mismatch of the model and the empirical structure of traffic states is even more obvious for the OV-function (Fig. 4.12). It shows almost no density dependence and is basically independent of the traffic state. The difference between the different curves is only in a density dependent cut-off of the distribution, i.e., at large densities large distances simply do not occur.
Compared to the empirical setup used in this chapter, the simulation results of the HS model reveal that the straightforward implementation of OV-curves leads to a total density determination of the vehicle dynamics, independent of the traffic state. Moreover, the deterministic behavior is in contradiction to empirical observations. In particular, for a proper choice of λ the vehicles take instantaneously the optimal velocity and, thus, the dynamical aspects of highway traffic are extremely simplified. This leads to a very strong tendency of the model to produce homogeneous traffic states, which is in sharp contrast to the observed complexity of traffic states.

4.4 The BL model

The previous sections have shown that the present CA models do not provide a satisfactorily description of the synchronized state, and that especially the empirical findings of the velocity distance-headway relationship and the time-headway distribution cannot be reproduced. However, the TOCA, the ER and the HS model try to improve the degree of realism in modeling traffic flow by increasing the interaction horizon of a vehicle which in the NaSch and the VDR model is restricted to $v_{\max}$ cells. Unfortunately, the way the interaction of the vehicles is implemented is static and leads to a total determination of the driving behavior by the density. By means of a dynamical response, on the contrary, vehicles are able to adjust their velocity according to the actual traffic situation, regardless of the traffic density in front.

Thus, in order to implement a dynamical interaction of the vehicles that allows to capture the elementary vehicle dynamics in the various traffic states (see chapter 3), in this section the set of update rules of the NaSch model [80, 82] is extended to a driving strategy that comprises four aspects:

(i) At large distances the cars move (apart from fluctuations) with their desired velocity $v_{\max}$.

(ii) At intermediate distances, drivers react to velocity changes of the next vehicle downstream, i.e., to "brake lights" [35].

(iii) At small distances, the drivers adjust their velocity such that safe driving is possible.

(iv) The acceleration is delayed for standing vehicles and directly after braking events.

The model combines several elements of recent modeling approaches, e.g., velocity anticipation [10, 79] and a slow-to-start rule [8]. While the slow-to-start rule allows to adjust the upstream velocity of a wide jam, vehicles are able to reduce the time-headway to their predecessor considerably by anticipating the predecessor's movement in the next time-step. In addition to that, a dynamical long ranged interaction is included: In their velocity dependent interaction horizon, drivers react on brakings of the leading vehicle that are indicated by an activated brake light [35]. The interaction, however, is limited to nearest neighbor vehicles [50]. This kind of event-driven anticipation enables a vehicle to reduce its velocity timely when approaching a jam. The implementation used in the simulation allows the upstream propagation of the brake light, which turns out to be crucial for modeling synchronized traffic.
The update rules of the NaSch model with brake lights (BL model) are formulated in analogy to the VDR model. In particular the interactions are strictly local, and a parallel update scheme is applied.
Before the introduction of the update rules, the most important quantities are defined. In the following, the position and velocity of the n-th car at time t is denoted by $x_n(t)$ and $v_n(t)$, respectively. Cars are numbered in driving direction, i.e., vehicle $n+1$ precedes vehicle n. A car may occupy more than a single cell. Therefore the gap between consecutive cars is given by $d_n = x_{n+1} - x_n - l$ (where l is the length of the cars). The brake light b_n can take on two states, i.e., on (off) $\rightarrow b_n = 1(0)$. In the approach, the randomization parameter p_{dec} for the n-th car can take on three different values p_0, p_d and p_b, depending on its current velocity $v_n(t)$ and the status $b_{n+1}(t)$ of the brake light of the preceding vehicle $n+1$:

$$p_{\text{dec}} = p_{\text{dec}}(v_n(t), b_{n+1}(t), t_n^h, t^s) = \begin{cases} p_b & \text{if } b_{n+1}(t) = 1 \text{ and } t_n^h < t^s \\ p_0 & \text{if } v_n(t) = 0 \\ p & \text{in all other cases.} \end{cases} \tag{4.8}$$

The two times $t_n^h = \frac{d_n^{(\text{eff})}}{v_n}$ (if $v_n = 0$ then $t_n^h = \infty$) and $t^s = \min(v_n, h)$, where h determines the range of interaction with the brake light, are introduced to compare the time t_n^h needed to reach the position of the leading vehicle with a velocity-dependent (temporal) interaction horizon t^s. t^s introduces a cutoff that prevents drivers from reacting to the brake light of a predecessor that is very far away. Finally $d_n^{(\text{eff})} = d_n + \max(v_{\text{anti}} - d_{\text{security}}, 0)$ denotes the *effective* gap where $v_{\text{anti}} = \min(d_{n+1}, v_{n+1})$ is the expected velocity of the leading vehicle in the next time step. The effectiveness of the anticipation is controlled by the parameter d_{security}. Accidents are avoided only if the constraint $d_{\text{security}} \geq 1$ is fulfilled. The update rules then are as follows:

0. *Determination of the randomization parameter:*
   $p_{\mathrm{dec}} = p_{\mathrm{dec}}(v_n(t), b_{n+1}(t), t_n^h, t^s)$
   $b_n(t+1) = 0$

1. *Acceleration:*
   if $((b_{n+1}(t) = 0)$ and $(b_n(t) = 0))$ or $(t_n^h \geq t^s)$ then:
   $v_n\left(t + \frac{1}{3}\right) = \min(v_n(t) + 1, v_{\max})$

2. *Braking rule:*
   $v_n\left(t + \frac{2}{3}\right) = \min\left(v_n\left(t + \frac{1}{3}\right), d_n^{(\mathrm{eff})}\right)$
   if $(v_n\left(t + \frac{2}{3}\right) < v_n(t))$ then:
   $b_n(t+1) = 1$

3. *Randomization, brake:*
   if $(\mathrm{rand}() < p_{\mathrm{dec}})$ then:
   - $v_n(t+1) = \max\left(v_n\left(t + \frac{2}{3}\right) - 1, 0\right)$
   - if $(p_{\mathrm{dec}} = p_b)$ then:
     $b_n(t+1) = 1$

4. *Car motion:*
   $x_n(t+1) = x_n(t) + v_n(t+1)$

The velocity of the vehicles is determined by steps $1-3$, while step 0 determines the dynamical parameter of the model. Finally, the position of the car is shifted in accordance to the calculated velocity in step 4.
In order to illustrate the details of the approach, the update rules are now discussed step-wise.

0) The braking parameter p_{dec} is calculated. For a car at rest, the value $p_{\mathrm{dec}} = p_0$ is applied. Therefore p_0 determines the upstream velocity of the downstream front of a jam.

   If the brake light of the car in front is switched on, and is the car is found within the interaction horizon, $p_{\mathrm{dec}} = p_b$ is chosen. A car perceives a brake light of the vehicle ahead within a time dependent interaction horizon $t^s = \min(v_n(t), h)$ where $v_n(t)$ is the current velocity and h an integer constant. The velocity dependence takes into account the increased attention of the driver at large and reduces the braking readiness at small velocities. This reaction is performed only with a certain probability of p_b. In order to obtain finite interactions, a cutoff at a horizon of h seconds is made [4].

   Finally, $p_{\mathrm{dec}} = p$ is chosen in all other cases.

[4] Indeed, increasing p_{dec} to p_b is the simplest possible response to the stimulus brake light. More sophisticated response functions like a direct reduction of the velocity or the gap are conceivable but lead to some problems in combination with anticipation. In addition, one can think of different implementations of the brake noise p_b. For example, one may chose more sophisticated p_b-functions, like a linear relationship of p_b and the velocity, the difference velocity to the predecessor or the gap, but for the sake of simplicity it is focused on a constant p_b.

1) The velocity of the car is enhanced by one unit if the car does not already move with the maximum velocity. The car does not accelerate if its own brake light or that of its predecessor is on and if the next car ahead is within the interaction horizon.

2) The velocity of the car is adjusted according to the effective gap.

   The brake light of a vehicle is activated only if the velocity is reduced compared to the preceding time-step. The comparison of the velocity of the vehicle with its old velocity avoids artificial brake lights due to an acceleration in step 1 and a following deceleration in step 2: Suppose the brake light would be calculated in the NaSch braking rule, that is if the braking rule is applied. If a car accelerates now in step 1 but decelerates in step 2 by one unit, its velocity remains unchanged, but the brake light will be activated.

3) The velocity of the car is reduced by one unit with a certain probability $p_{\text{dec}} = p_{\text{dec}}(v_n(t), b_{n+1}(t), t_n^h, t_s)$. If the car brakes due to the predecessor's brake light, its own brake light is switched on.

4) The position of the car is updated.

The parameters of the model that allow to adjust the simulation data to the empirical findings are the following: the maximal velocity $v_{\max}$, the car length l, the braking parameters p, p_b, p_0, the cut-off time of interactions h and the minimal security gap d_{security}.
In order to obtain realistic values of the acceleration behavior of a vehicle, the cell length of the standard CA model is reduced to a length of 1.5 m. Since the time-step is kept fixed at a value of 1 s, this leads to a velocity discretization of 1.5 m/sec which is of the same order as the "comfortable" acceleration of somewhere about 1 m/sec^2 [135]. Like in the standard CA model, a vehicle has a length of 7.5 m that corresponds to 5 cells at the given discretization (see appendix B for a discussion of the discretization effects).
Some of the parameters can be fixed as, e.g., in the VDR-model: The maximum velocity $v_{\max}$ is determined by the slope of the free flow branch of the fundamental diagram. Because the empirical data is collected on a highway with a (theoretically) speed limit of 100 km/h, v_{max} is set to 20 cells/time-step = 108 km/h. The upstream velocity of a jam can be tuned by the parameter p_0, and the strength of fluctuations that are controlled by the parameter p_d determine the maximal flow.
The other parameters of the model are connected with an interaction that has not been included in the models discussed so far. The parameter h describes the horizon above that driving is not influenced by the leading vehicle. Several empirical studies reveal that h corresponds to a *temporal* headway rather than to a spatial one. The estimations for h vary from 6 s [34], 8 s [100, 128], 9 s [51] to 11 s [26]. Another estimation for h can be obtained from the analysis of the perception sight distance. The perception sight distance is based on the first perception of an object in the visual field at which the driver perceives a movement (angular velocity). In [113] velocity-dependent perception sight distances are presented that, for velocities up to 128 km/h, are larger than 9 s. Therefore h is set to 6 s as a lower bound for the time-headway. Besides, the simulations show that correct results can only be obtained for $h \geq 6$. This corresponds to a maximum horizon of 6×20 cells, or a distance of 180 m, at velocity $v_{\max}$.
The next parameter one has to fix is p_b. This parameter controls the propagation of the brake light. A braking car in front is indeed a strong stimulus to adjust the own speed. Therefore p_b has typically a high value. Finally, d_{security} tunes the degree of the velocity anticipation and has a strong influence on the cut-off of the time-headway distribution.

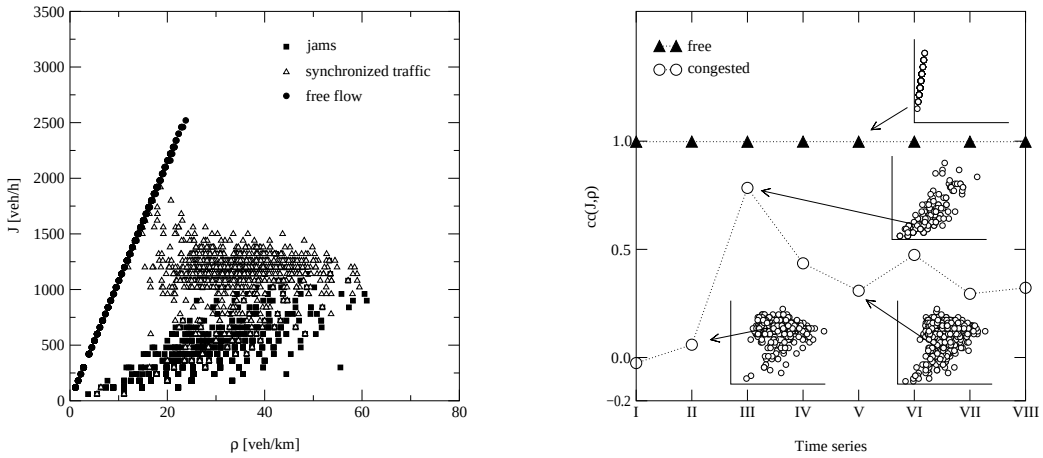

Figure 4.13: Left: Local fundamental diagram obtained by the simulation of the BL model. The parameters are: $p_0 = 0.5$, $h = 6$, $v_{\max} = 20$, $p = 0.1$, $p_b = 0.94$, $d_{\text{security}} = 7$. A time-step corresponds to 1 s, a cell has a length 1.5 m and a vehicle covers 5 cells. Right: Crosscorrelation of the flow and the density in free flow and congested traffic for different densities and homogeneous initialization.

4.4.1 Validation of the BL model

With this parameter set the model is calibrated to the empirical data. Leaving h and $v_{\max}$ fixed, the best agreement with the empirical data can be achieved for $p = 0.1$, $p_b = 0.94$, $p_0 = 0.5$ and $d_{\text{security}} = 7$.
As one can see in Fig. 4.13, the slope of the free flow branch and the maximum flow coincide with the empirical data indicating that $v_{\max}$ and p have been chosen properly.
However, the simulated densities are less distributed than in the empirical data set. As mentioned earlier, this observation is simply an artifact of the discretization of the velocities that determines the upper limit of detectable densities.
A second lower branch appears for small values of the flow which represents wide jams. Because only moving cars are measured by the inductive loop, large densities cannot be calculated.
The next parameter that can be directly related to an empirical observable quantity, namely the upstream velocity of the downstream front of a wide jam, is the deceleration probability p_0.
The velocity of the jam front is determined by the calculation of the density autocorrelation function in the congested state of a system that was initialized with a mega jam. As a result, one obtains an average jam velocity of 2.36 cells/time-step ($\triangleq$ 12.75 km/h) for $p_0 = 0.5$. This jam velocity is independent of the traffic condition and holds for all densities in the congested regime. Thus, although meta-stable traffic states can be achieved by the finer discretization (see appendix B), the slow-to-start rule is necessary for the reduction of the jam velocity from about 20.45 km/h to 12.75 km/h. This velocity is also in accordance with empirical results [63].
A more detailed statistical analysis [110] of the time-series of flux, velocity and density

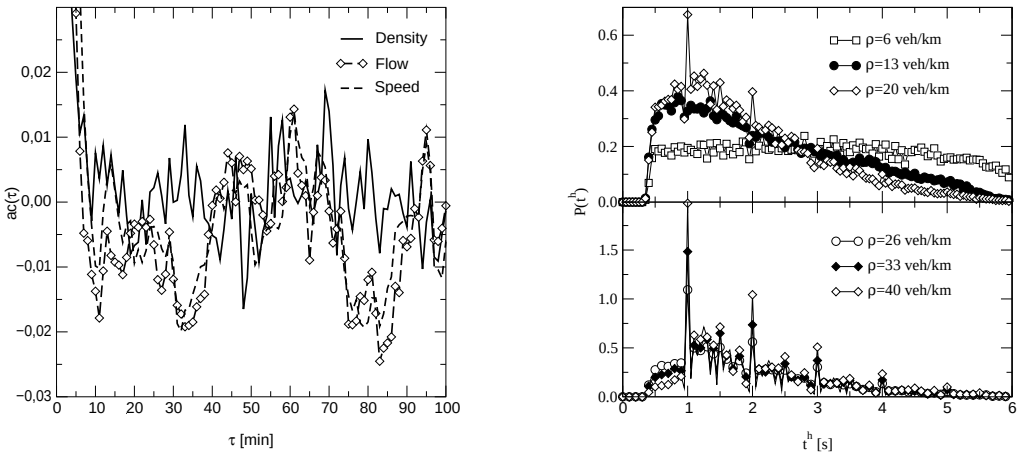

Figure 4.14: Left: Autocorrelation function of the density, the velocity and the flow for a density of 67 veh/km with a random initialization. Right: Time-headway distribution for different density regimes in free flow (top) and in the synchronized state (bottom).

allows the identification of three different traffic states [63, 67, 78]. Following the arguments of [110], free flow and congested states can be identified by means of the average velocity. A contiguous time-series of minute averages above 90 km/h was classified as free flow, otherwise as congested flow. In Fig. 4.13, the cross-covariance $cc(J, \rho)$ of the flow and the local measured density for different traffic states is shown. In the free flow regime the flow is strongly coupled to the density, indicating that the average velocity is nearly constant. Also for large densities, when wide jams are measured, the flow is mainly controlled by density fluctuations. In the mean density region there is a transition between these two regimes. At cross-covariances in the vicinity of zero, the fundamental diagram shows a plateau. Traffic states with $cc(J, \rho) \approx 0$ are identified as synchronized flow [110]. In the further comparison of the simulation with the corresponding empirical data, these traffic states are used for synchronized flow data and congested states with $cc(J, \rho) \gg 0.7$ for data of wide jams. The results indicate that the approach leads to realistic results for the fundamental diagram and that the model is able to reproduce the three different traffic states.

To characterize the three traffic states, the autocorrelation function of the flow, the density as well as the velocity for different densities is calculated. In free flow, the same oscillations of the autocorrelation function of the density and the flow can be observed, whereas the speed is not correlated in time. In contrast to the NaSch model, the autocorrelation function at large densities is characterized by a strong coupling of the flow and the velocity. Now, the velocity of a car not only depends on the gap but also on the density, so that the flow and the velocity are mainly controlled by the density. (Fig. 4.14).

Next the empirical data and simulation results are compared on a microscopic level. In Fig. 4.14, the simulated time-headway distributions for different density regimes are represented. Due to the discrete nature of the model, large fluctuations occur, and the continuous part of the empirical distribution shows a peaked structure at whole-numbered head-

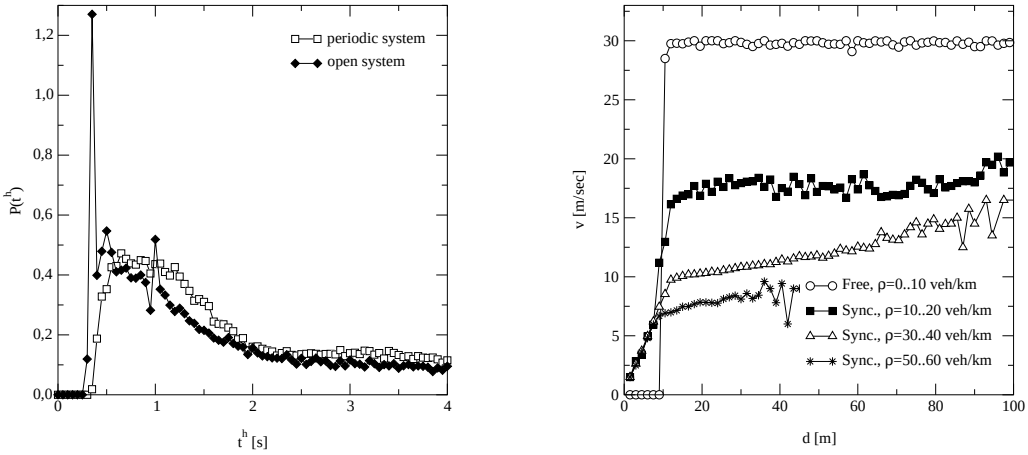

Figure 4.15: Left: Time-headway distribution in the free flow regime of a system with open boundary conditions and different types of vehicles. The maximal velocity of the slow vehicles was set to $v_{\max} = 108$ km/h $= 20$ cells/time-step and of the fast vehicles to $v_{\max} = 135$ km/h $= 25$ cells/time-step. 15% of the vehicles are considered as fast vehicles (note that these are vehicles that disregard the speed limit). Right: The mean speed chosen by the driver as a function of the gap to his predecessor for free flow and congested traffic and different densities.

ways for the simulations. In the free flow state, extremely small time-headways have been found, in accordance with the empirical results. Nevertheless, for the standard simulation setup at small densities, the statistical weight of these small time-headways is significantly underestimated. Therefore simulations of an open system with different types of vehicles are performed. Fig. 4.15 demonstrates that the origin of the maximum of the distribution at small time-headways are fast cars driving in small platoons behind slow vehicles. The location of this maximum is mainly influenced by the parameter d_{security}. The results for congested flow, however, are not influenced by different types of vehicles.
The ability to anticipate the predecessor's behavior becomes weaker with increasing density so that the weight of the small time-headways is reduced considerably in the synchronized state. The maximum of the distribution can be found in the vicinity of 1 s in accordance with the empirical data, the density dependence, however, cannot be reproduced. Instead, with increasing density, the maximum at a time of 1 s (in the NaSch model the minimal time headway is restricted to 1 s because of rule 2) becomes more pronounced. This result is also due to the discretization of the model that triggers the spatial and temporal distance between the cars. Because of the exponential decay of the waiting time distribution of cars leaving a jam, the peak at a time of 1 s is the most probable in the time-headway distribution.
The OV-curve of the model approach shows an excellent agreement with empirical findings. For densities in the free flow regime it is obvious that the OV-curve (Fig. 4.15) deviates from the linear velocity-headway curve of the NaSch model.
Due to anticipation effects, smaller distances occur, so that driving with $v_{\max}$ is possible even within very small headways. This strong anticipation becomes weaker with increasing

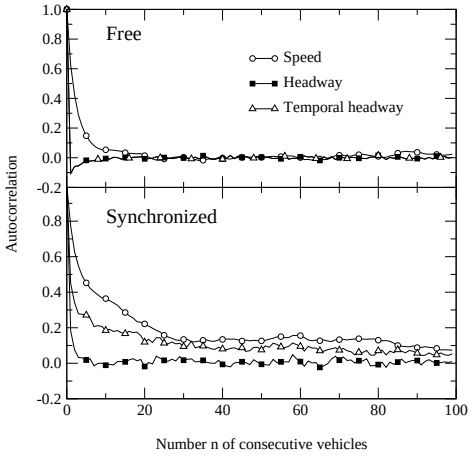

Figure 4.16: Autocorrelation of the speed and of the spatial and temporal headway for free flowing vehicles (top) and for a synchronized state (bottom). In order to obtain a slow decay of the speed autocorrelation function in the free flow regime the simulation was performed with an open system with 20% slow cars ($v_{\max}^{\text{slow}} = 15$ cells/time-step $= 81$ km/h, $v_{\max}^{\text{fast}} = 20$ cells/time-step $= 108$ km/h.)

density, and cars tend to have smaller velocities than the headway allows so that the OV-curve saturates for large distances. The saturation of the velocity, that is characteristic for synchronized traffic, was not observed in earlier approaches. The value of the asymptotic velocities can be adjusted by the last free parameter p_b. The OV-curve in the synchronized regime is independent of the maximum velocity and is only determined by the dynamical behavior of the model.
Next, the autocorrelation of the time-series of the single-vehicle data is calculated in Fig. 4.16. Note that the data of the free flow state was collected in an open system with 20% of slow cars with $v_{max} = 15$ cells/time-step $= 81$ km/h. In the free flow regime, a strong coupling of the spatial and temporal headway can be observed that supports the results obtained by aggregated data ($J \propto 1/t^h$ and $\rho \propto 1/d$). In contrast, the autocorrelation of the velocity indicates a slow asymptotic decay. This supports the explanation of [110] that the slow decrease for small distances is due to small platoons of fast cars led by one slow car. In the synchronized state, longer correlations of the speed and the spatial headways can be observed. So, similar to the free flow regime, in the synchronized regime, platoons of cars that are moving with the same speed appear .

4.5 Comparison of the models

The comparison of the models presented so far is based on local measurements of inductive loops. Therefore, the model parameters have been chosen in order to allow the best possible accordance with the empirical setup. One of the main disadvantages of local measurements, however, is that the detected values of the flow and the velocity strongly fluctuate whereas density cannot be defined locally in a strict sense. In contrast, by means of traffic flow

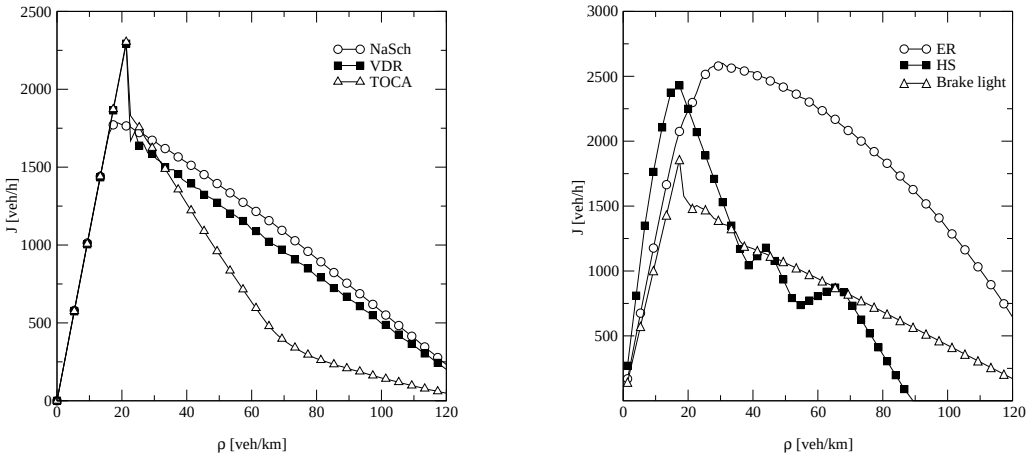

Figure 4.17: Comparison of the global fundamental diagram of the discussed models for typical parameter values and a homogeneous initialization.

simulations it is possible to get averaged quantities that are representative for a given density. Due to this fact, in this section global measurements of the flow and the density of the various models are given for a typical set of parameters in order to demonstrate the characteristics of the approaches. However, since density can be exactly calculated, the distinction between the traffic states is omitted. Density, flow and velocity can be measured globally via equation (2.10), equation (2.12) and equation (2.11) as discussed in section 2.1.

A fundamental diagram, in general, consists of a linear free flow branch that intersects with a linear congested branch at the density of maximum flow. As one can see in Fig. 4.17, nearly all discussed models are able to reproduce this basic characteristics. The fundamental diagram of the HS model, however, exhibits two distinct maxima. The first maximum is simply given by the transition from free flow to congested traffic. The second maximum is a consequence of the chosen OV-curve. Since vehicles with $3 \leq d \leq 5$ have to drive with a velocity of 2, the flow increases linearly for densities well above a certain density until the average gap is smaller than 3 cells. Moreover, due to the OV-curve, the vehicles behave deterministically and chose their velocity according to the gap. As a result of a nearly uniform gap distribution, speed limits are applied for certain density intervals, and different slopes in the congested branch of the fundamental diagram become visible.

This behavior can also be found in the ER model. Since the choice of the gap-velocity matrix in the ER model leads to speed limits for different density regimes, the free flow branch shows two different slopes like in the local measurements. But more important than that is the lack of a distinct maximum in the fundamental diagram. This is a consequence of the ordered sequential update of the ER model. It is possible that jams can also move in downstream direction, thus, leading to many small jams with a large flow.

Measurements of empirical data have revealed that the outflow from a jam is reduced considerably compared to the maximum possible flow. As a result, meta-stable free flow states exist, and hysteresis effects can be observed in the fundamental diagram.

Obviously, this is the case for the VDR model, the TOCA model as well as for the BL

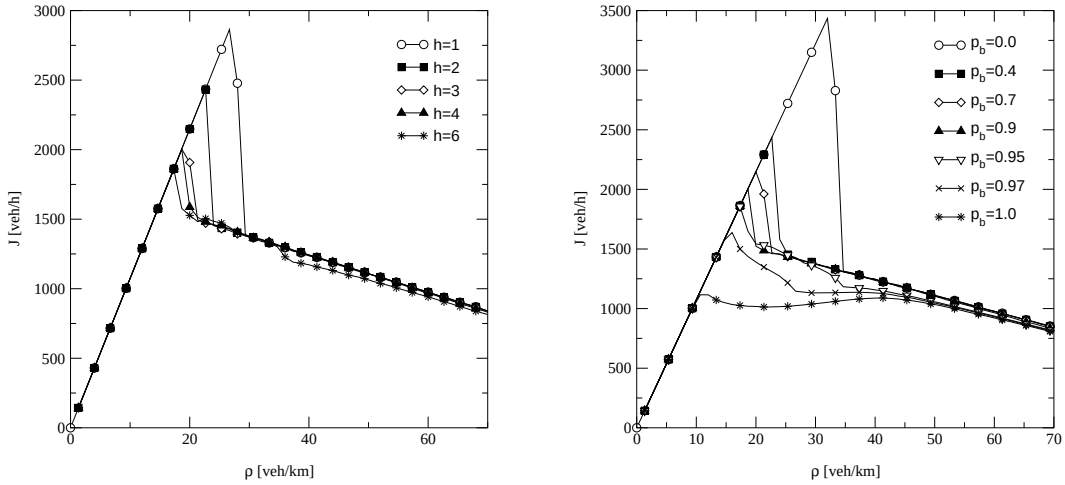

Figure 4.18: Fundamental diagram for different horizons h (left) and different p_b (right) with homogeneous initialization.

model while the maximum possible flow of the NaSch model is as large as the outflow from a jam. Since the deceleration probability in the VDR model was chosen very small ($p_{dec} = 0.01$), the stability of the homogeneous branch of the fundamental diagram is very large. In contrast, once a jam has formed above a certain threshold density, the large deceleration probability for the vehicles at rest is responsible for the reduced outflow from a jam. As a result, the system is phase separated into a region of free flow and a compact moving jam. The capacity drop can simply be tuned by varying the difference between the two deceleration parameters. In analogy to the VDR model, in the TOCA model only vehicles with $v \leq d$ decelerate with the probability p_{dec}. Thus, vehicles driving with $v_{\max}$ and $d > v$ lead to a stable high flow branch in the fundamental diagram up to a density of $\frac{1}{v_{\max}+1}$. But more important than that is that in the congested regime the TOCA model reveals the existence of two different slopes in the fundamental diagram. For densities larger than $1/2 = 66$ veh/km, vehicles have on average a gap of less than one cell. Since the vehicles decelerate with a large probability but do accelerate with a rate smaller than one, the system now contains only one large jam whose width is comparable to the system size.

Like in the VDR model, in the BL model the high flow states can simply be controlled by the deceleration parameter p_0 for vehicles at rest. However, in the congested regime, two distinct slopes of the fundamental diagram become visible. The density at which the slope changes and the shape of the fundamental diagram can be triggered by the parameters h and p_b that determine the interaction between vehicles with $d > v$. In particular, the higher h, the smaller the density $\rho_{\max}$ of the maximum flow (Fig. 4.18). For large h the fundamental diagram converges very fast so that the fundamental diagram for values larger than $h = 8$ are identical. Moreover, even small values of p_b have a strong influence on the flow. The high flow branch of the fundamental diagram (Fig. 4.18) and the density $\rho_{\max}$ of maximum flow are reduced. For large values, two different slopes of the congested branch can be observed in the fundamental diagram. The higher p_b, the smaller the density at which the slope changes.

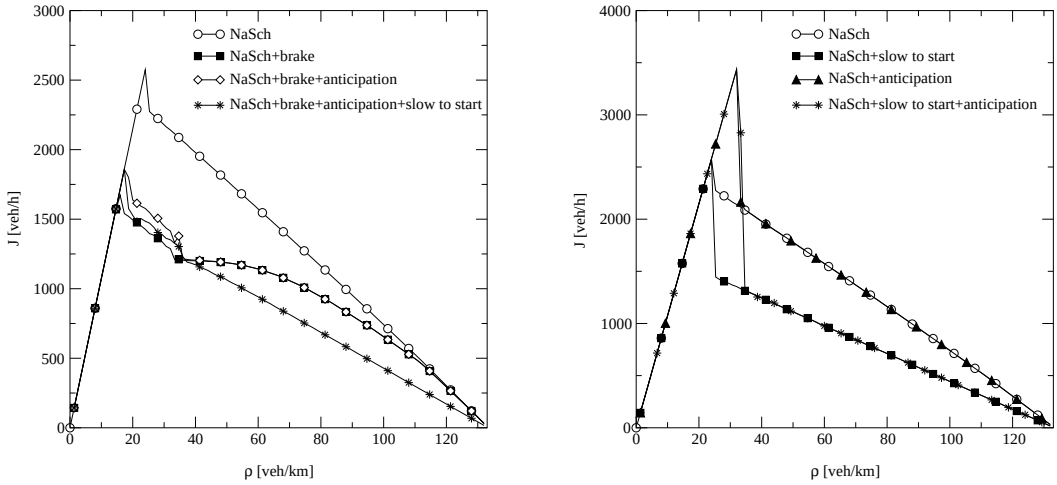

Figure 4.19: Successive extension of the NaSch model with (left) and without (right) brake lights. Note that the system is initialized homogeneously to view high flow states.

4.5.1 Reduction of the BL model

The BL model shows an excellent agreement with the empirical data, especially in the case of the OV-curve. Nevertheless, this is only possible with the application of a variety of new update rules. Therefore, it remains an open question whether this set of update rules can be reduced.
In Fig. 4.19, the extensions of the model are successively dropped. First, the slow-to-start rule has been omitted. Without the slow-to-start rule, the model lacks the ability of a reduced outflow from a jam, and the number of large compact jams is reduced so that the flow increases. As a further reduction of the model, anticipation is switched off. This leads to a decrement of the flow at densities larger than the density of the maximum flow. Now headways smaller than the velocity are not possible, which manifests in the OV-curve at small densities. For large densities, the anticipation of the velocity of the predecessor becomes more and more difficult until anticipation is no longer applicable. Therefore, the differences between the curves with and without anticipation vanishes.
Applying the braking rule as the only extension leads to a plateau-like fundamental diagram compared to the NaSch model. Additionally, the flow is reduced dramatically. It is the braking rule that changes the shape of the fundamental diagram.
In Fig. 4.19, the same successive reductions of the rules have been applied to the model without the braking rule. Neither the anticipation, nor the slow-to-start rule applied as a single extension or in combination are able to change the shape of the fundamental diagram.
Considering the empirical fact that small time headways and a reduced outflow from a jam exist, the braking rule is the only new extension of the NaSch model. This new rule turns out to be crucial for the correct generation of the OV-curves and the occurrence of synchronized traffic.

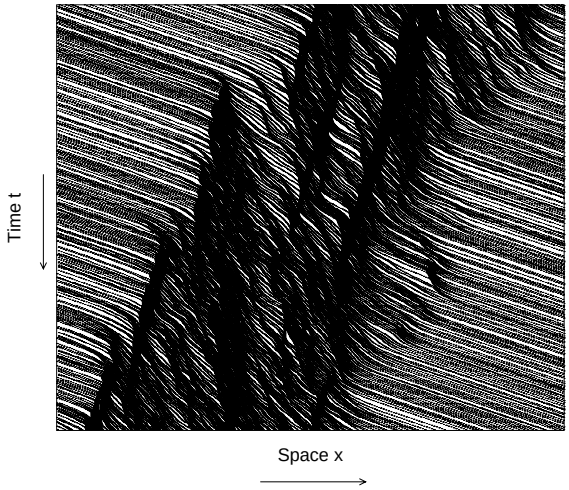

Figure 4.20: Space-time plot of a periodic system for a global density of 27 veh/km. The cars are moving from left to right. Note that the cars have a length of 5 cells. Each dot represents a vehicle. For the sake of illustration only the front of a vehicle is visualized.

4.6 Discussion

The comparison of the Nagel and Schreckenberg model with some of its variants has revealed that differences between the models can be found on a macroscopic scale, but that these differences are even more pronounced on a microscopic level of description. It turns out that the BL model shows the best agreement with the empirical test scenario. Anyhow it is important to know which aspects of real traffic are described by a certain model. In the end, the aspired accordance of a model with empirical observations strongly depends on the goal of the particular application. So it is useful to use oversimplified model approaches in order to concentrate on particular aspects of traffic flow phenomena [103].
In section 4.5 it was shown that the ER and the HS model fail to produce a realistic fundamental diagram. In the case of the ER model, the sequential update scheme is responsible for a totally unrealistic jam dynamics, i.e., jams moving in downstream direction can be observed. The dynamics of the HS model is determined by the special choice of the OV-curve. As a consequence, it is not possible to obtain a fundamental diagram that exhibits one maximum of flow.
The NaSch model, the VDR model, the TOCA model and the BL model reproduce the fundamental diagram quite well. In urban traffic, for example, the dynamics of the vehicles between two intersections is predominantly determined by traffic lights. The correct description of queues at cross-roads, therefore, only requires the existence of two distinct traffic phases, namely free flow and congested traffic.
More realistic applications of traffic flow simulations, e.g., that allow the tracing of a jam, need a more detailed description of the jamming mechanisms. For the correct reproduction of the upstream propagation of the downstream front of a jam, it is necessary to reduce the outflow from a jam and thus to facilitate meta-stable states. Here, the VDR model, the TOCA model and the BL model allow the existence of states with a flow considerably larger than the outflow from a jam.
Differences between the models can be observed in the jam dynamics. While the road

in the VDR model is separated into a region with free flow and a compact jam that propagates upstream, the peculiarities of the update rules of the TOCA model lead to a jam that covers the whole system.
Large compact jams appear also in the BL model since the slow-to-start rule of the VDR-model is included. However, brake lights are responsible for the generation of synchronized regions, i.e., regions of vehicles that are moving with a small velocity but a large headway. This difference in the vehicle dynamics becomes most obvious in the analysis of locally measured single-vehicle data. As a consequence of the increased set of update rules, the BL model gives the most satisfying agreement with the empirical observations.
On a microscopic level of description, it turns out that the main difficulty in the realistic modeling of highway traffic lies in the reproduction of small time-headways that can be found at low densities in free flow and in the density dependence of the velocity-distance relationship. This important behavior of the OV-curve demonstrates that the driving strategy of a vehicle depends strongly on the traffic state, while the vehicles of most of the model approaches adjust their velocity directly to their gap in front.
However, it turns out that as a first step towards a realistic modeling of highway traffic the interaction horizon of the original NaSch model has be to enhanced like in the TOCA, the ER and the HS model. Unfortunately, the TOCA model did not decrease the cell length, which is necessary in order to reproduce realistic acceleration values while in the HS model vehicles can accelerate to $v_{\max}$ within one time-step. Therefore, the benefits of the increased interaction horizon do not become visible. Moreover, vehicles do react in a static manner to a stimulus within the horizon. In particular, the velocity gap matrix used in the ER model just leads to speed limits for certain densities. Especially the HS model demonstrates the shortcomings of a driving strategy totally determined by the gap in front and, therefore, by the density. A dynamical response, on the contrary, will enable the vehicles to adjust their velocity to the actual traffic situation regardless of the traffic density in front.
This idea of event-driven anticipation is incorporated in the BL model. It turns out that only the introduction of the brake lights that allow the timely adjustment of the velocity of a vehicle to the downstream speed and that propagate in upstream direction allows the reproduction of synchronized traffic. The calculation of an effective gap by means of velocity anticipation, on the contrary, reduces velocity fluctuations in free flow and leads to platoons of vehicles driving bumper-to-bumper.
As a result, simulations of the BL model show that the empirical data are reproduced in great detail. In particular, three qualitatively different microscopic traffic states that are in accordance with the empirical results can be observed (see the space-time plot in Fig. 4.20). The deviations of the simulation results are mainly due to simple discretization artifacts which do not reduce the reliability of the simulation results. It has also to be stressed that the agreement manifests on a microscopic level. This improved realism of the BL model leads to a larger complexity of the approach compared to other models of this type. Nevertheless, due to the discreteness and the local car-car interactions, very efficient implementations should still be possible. Moreover, the adjustable parameters of the model can directly be related to empirical quantities. The detailed description of the microscopic dynamics will also lead to a better agreement of simulations with respect to empirical data for macroscopic quantities, e.g., jam-size distributions. Therefore this approach should allow more realistic micro-simulations of highway networks.